ELSEVIER

Comput. Methods Appl. Mech. Engrg. 190 (2001) 6141–6155

Computer methods in applied mechanics and engineering

www.elsevier.com/locate/cma

An AIM and one-step Newton method for the Navier–Stokes equations ☆

Kaitai Li *, Yanren Hou

College of Science, Xi'an Jiaotong University, Xi'an 710049, People's Republic of China

Received 10 November 1999

Abstract

In this paper, we investigate a two-level finite element approximation to the Navier–Stokes equations by means of a new approximate inertial manifold (AIM). Then we construct a new AIM-based numerical scheme and show that the convergence rate of the new approximation obtained by this AIM method is better than the double of the convergence rate of the standard Galerkin finite element solution. In addition, we also show that the new AIM scheme is equivalent to a one-step Newton iterative scheme for the Navier–Stokes equations in a suitable Hilbert space. © 2001 Elsevier Science B.V. All rights reserved.

MSC: 65N30; 76D05

Keywords: Finite element; The Navier–Stokes equations; Two-level method

1. Introduction

There have been a lot of interests recently in developing the higher-order finite element methods for solving the boundary and initial-boundary value problems of partial differential equations. For example, the superconvergent finite element methods, the multi-level finite element methods and the nonlinear Galerkin method, etc. We refer the readers to Lin [10], Marion and Temam [11], Garcia-Achilla et al. [5], Layton and Lenferink [8,9], Xu [13,14], Marion and Xu [12] and the references therein for details.

In this paper, we are interested in applying the two-level technique associated with the concept of the approximate inertial manifold (AIM) to construct the high order finite element scheme for the steady Navier–Stokes equations. The crucial point of the construction of our new two-level scheme is to find a new approximate inertial manifold which can better reflect the interaction between the higher frequency and the lower frequency components of the solution to the Navier–Stokes equations than other AIMs at hand. In fact, the two-level methods developed from this AIM approach are not called that, but rather AIM scheme or nonlinear Galerkin scheme.

Assume that $(\boldsymbol{u},p)\in Y$, (a Sobolev space), is the true solution and Y_h is a finite element subspace of Y. We will construct a crucial projection (Q_h,R_h) mapping any function from Y onto Y_h. Then we can decompose the true solution as follows:

$$(\boldsymbol{u},p)=(Q_h(\boldsymbol{u},p),R_h(\boldsymbol{u},p))+(\hat{\boldsymbol{u}},\hat{p}),$$

☆ Subsidized by the special funds for major state basic research projects G1999032801-07. The second author is also supported by the research funds of Tianyuan Mathematics and Xi'an Jiaotong University.

* Corresponding author. Tel.: +86-29-2669051; fax: +86-29-3237910.
E-mail address: ktli@xjtu.edu.cn (K. Li).

PII: S0045-7825(01)00213-4

where $(\hat{\boldsymbol{u}}, \hat{p}) \in \hat{Y}_h$ and $\hat{Y}_h$ is an orthogonal complement of Y_h with respect to a certain scalar product. Normally, the projection $(Q_h(\boldsymbol{u},p), R_h(\boldsymbol{u},p))$ contains the lower frequency components of the solution $(\boldsymbol{u},p)$ while $(\hat{\boldsymbol{u}}, \hat{p})$ contains the higher frequency components.

Let $(\boldsymbol{u}_h, p_h)$ be the standard Galerkin finite element approximation to the Navier–Stokes equations. Our error analysis shows that the error between $(Q_h(\boldsymbol{u},p), R_h(\boldsymbol{u},p))$ and $(\boldsymbol{u}_h, p_h)$ is of higher-order comparing with the error between $(\boldsymbol{u},p)$ and $(\boldsymbol{u}_h, p_h)$. Using the previous decomposition of $(\boldsymbol{u},p)$, we have

$$|||(\boldsymbol{u}_h - \boldsymbol{u}, p_h - p)||| \leqslant |||(\boldsymbol{u}_h - Q_h(\boldsymbol{u},p), R_h(\boldsymbol{u},p) - p_h)||| + |||(\hat{\boldsymbol{u}}, \hat{p})|||,$$

where $|||\cdot|||$ is the graph norm in Y to be specified later. Note that $|||(\hat{\boldsymbol{u}}, \hat{p})|||$ is the error due to projection, which is the truncated part of the solution with respect to our projection and is a small quantity of lower order. That is the error of the standard Galerkin approximation is dominated by this truncated term.

Our main idea is that if there exists a Lipschitz continuous mapping $\Phi = (\boldsymbol{\phi}, \xi)$: $Y_h \to \hat{Y}_h$ such that

$$|||(\hat{\boldsymbol{u}} - \boldsymbol{\phi}(\boldsymbol{u}_h, p_h), \hat{p} - \xi(\boldsymbol{u}_h, p_h))||| \quad \text{and} \quad |||(\boldsymbol{u}_h - Q_h(\boldsymbol{u},p), R_h(\boldsymbol{u},p) - p_h)|||$$

both have the accuracy of higher orders, then

$$(\boldsymbol{u}_*, p_*) = (\boldsymbol{u}_h + \boldsymbol{\phi}(\boldsymbol{u}_h, p_h), p_h + \xi(\boldsymbol{u}_h, p_h))$$

is a more accurate approximation to $(\boldsymbol{u},p)$ than $(\boldsymbol{u}_h, p_h)$. It is interesting that for this projection and Lipschitz mapping, the AIM scheme is equivalent to a one-step Newton iterative scheme, i.e., $(\boldsymbol{u}_*, p_*)$ is a solution of the linearized equations of the Navier–Stokes equations at $(\boldsymbol{u}_h, p_h)$.

Remark 1. This scheme can also be applied to the evolutionary Navier–Stokes equations which will be discussed in a coming paper of ours.

The contents of the paper are arranged as follows: we firstly consider the Navier–Stokes equations and its Galerkin finite element approximation in Section 2. Then we construct the crucial projection (Q_h, R_h): $Y \to Y_h$ and derive a lower frequency estimation in Section 3. In Section 4, we construct a new AIM, which is a Lipschitz continuous mapping Φ, and its related numerical scheme based on this projection and do some higher frequency analysis. Estimations show that the new scheme has much better convergence rate than that of standard Galerkin finite element solution. In Section 5, we demonstrate that the AIM-based numerical scheme is equivalent to a one-step Newton iterative method and give another equivalent form of the proposed scheme in Section 4 which is much easier to be carried out and therefore a high performance numerical scheme. Finally, for a test problem, we present some numerical results derived by our new scheme and some other numerical schemes, respectively, to verify the high performance.

2. Preliminaries

Consider the Navier–Stokes equations

$$\begin{cases} -\lambda\Delta\boldsymbol{u} + (\boldsymbol{u}\cdot\nabla)\boldsymbol{u} + \nabla p = \boldsymbol{f} & \text{in } \Omega, \\ \operatorname{div}\boldsymbol{u} = 0 & \text{in } \Omega, \\ \boldsymbol{u} = 0 & \text{on } \Gamma, \end{cases} \tag{2.1}$$

where $\Omega \subset R^d$, $d = 2$ or 3, is a bounded domain with a Lipschitz boundary Γ, $\boldsymbol{u}$ denotes the flow field, p is the pressure, $\boldsymbol{f}$ represents the exterior force which drives the flow and $\lambda = 1/Re$ with Re the Reynolds number.

We now introduce some notations. Set $Y = X \times M$, where $X = H_0^1(\Omega)^d$ and M is a subspace of $L^2(\Omega)$ defined by

$$M = L_0^2(\Omega) = \left\{ q : q \in L^2(\Omega),\ \int_\Omega q\,\mathrm{d}x = 0 \right\}.$$

The scalar product and norm in X are denoted by $((\boldsymbol{u},\boldsymbol{v})) = (\nabla\boldsymbol{u},\nabla\boldsymbol{v})$ and $\|\cdot\|$, while the scalar product and norm in M are denoted by the usual L^2 inner product and $|\cdot|$ respectively. Then the velocity–pressure variational formulation for (2.1) reads

$$\begin{cases} \text{find } (\boldsymbol{u},p)\in Y \quad \text{such that} \\ a(\boldsymbol{u},\boldsymbol{v}) + b(\boldsymbol{u};\boldsymbol{u},\boldsymbol{v}) - (p,\operatorname{div}\boldsymbol{v}) + (q,\operatorname{div}\boldsymbol{u}) = (\boldsymbol{f},\boldsymbol{v}) \quad \forall(\boldsymbol{v},q)\in Y, \end{cases} \tag{2.2}$$

where the bilinear form $a(\cdot,\cdot)$ and trilinear form $b(\cdot;\cdot,\cdot)$ are given by

$$a(\boldsymbol{u},\boldsymbol{v}) = \lambda((\boldsymbol{u},\boldsymbol{v})), \quad b(\boldsymbol{u};\boldsymbol{w},\boldsymbol{v}) = ((\boldsymbol{u}\cdot\nabla)\boldsymbol{w},\boldsymbol{v}) \quad \forall\boldsymbol{u},\boldsymbol{v},\boldsymbol{w}\in X.$$

Obviously, $a(\cdot,\cdot)$ is symmetric positive definite and continuous, i.e.,

$$|a(\boldsymbol{u},\boldsymbol{v})| \leqslant \lambda\|\boldsymbol{u}\|\,\|\boldsymbol{v}\|, \quad a(\boldsymbol{u},\boldsymbol{u}) \geqslant \lambda\|\boldsymbol{u}\|^2 \quad \forall\boldsymbol{u},\boldsymbol{v}\in X. \tag{2.3}$$

The trilinear form $b(\cdot;\cdot,\cdot)$ has the following properties [3]:

$$b(\boldsymbol{u};\boldsymbol{w},\boldsymbol{v}) = -b(\boldsymbol{u};\boldsymbol{v},\boldsymbol{w}) \quad \forall\boldsymbol{u}\in V, \ \ \boldsymbol{v},\boldsymbol{w}\in X, \tag{2.4}$$

$$|b(\boldsymbol{u};\boldsymbol{w},\boldsymbol{v})| \leqslant c_1\|\boldsymbol{u}\|_{s_1}\|\boldsymbol{w}\|_{s_2+1}\|\boldsymbol{v}\|_{s_1}, \tag{2.5}$$

where $c_1 > 0$ is a constant depending on the measurement of Ω,

$$V = \{\boldsymbol{v}\in X : (q,\operatorname{div}\boldsymbol{v}) = 0 \ \forall q\in M\},$$

and $\boldsymbol{u}\in H^{s_1}(\Omega)^d$, $\boldsymbol{v}\in H^{s_2}(\Omega)^d$, $\boldsymbol{w}\in H^{s_2+1}(\Omega)^d$ with $s_1\geqslant 0$, $s_2\geqslant 0$, $s_3\geqslant 0$ and

$$s_1+s_2+s_3 \geqslant \frac{d}{2}, \quad (s_1,s_2,s_3) \neq \left(0,0,\frac{d}{2}\right), \left(0,\frac{d}{2},0\right), \left(\frac{d}{2},0,0\right).$$

Inequality (2.5) will be used frequently in our later analysis. For the space, it is well known that it satisfies the following inf–sup condition for certain constant β_0:

$$\inf_{q\in M}\sup_{\boldsymbol{v}\in X}\frac{(q,\operatorname{div}\boldsymbol{v})}{|q|\,\|\boldsymbol{v}\|} \geqslant \beta_0 > 0. \tag{2.6}$$

We now consider the finite element approximation to the Navier–Stokes system (2.2). Assume that X_h and M_h are the finite element subspaces of X and M, respectively. Let I_h and J_h be the finite element interpolants associated with X_h and M_h, and we introduce the product space $Y_h = X_h\times M_h$, which is clearly a subspace of Y. Then the standard Galerkin finite element approximation is defined by

$$\begin{cases} \text{find } (\boldsymbol{u}_h,p_h)\in Y_h \quad \text{such that} \\ a(\boldsymbol{u}_h,\boldsymbol{v}) + b(\boldsymbol{u}_h;\boldsymbol{u}_h,\boldsymbol{v}) - (p_h,\operatorname{div}\boldsymbol{v}) + (q,\operatorname{div}\boldsymbol{u}_h) = (\boldsymbol{f},\boldsymbol{v}) \quad \forall(\boldsymbol{v},q)\in Y_h. \end{cases} \tag{2.7}$$

As usual, we make the following assumptions on the finite element subspace Y_h:

(H1) The approximation properties:

$$\inf_{(\boldsymbol{v}_h,q_h)\in Y_h}\{h\|\boldsymbol{u}-\boldsymbol{v}_h\| + |\boldsymbol{u}-\boldsymbol{v}_h| + h|p-q_h|\} \leqslant c\,h^{k+1}\{\|\boldsymbol{u}\|_{k+1} + \|p\|_k\}$$

for any $(\boldsymbol{u},p)\in Y\cap(H^{k+1}(\Omega)^d\times H^k(\Omega)), 1\leqslant k\leqslant l$.

(H2) Interpolation properties:

$$\|\boldsymbol{v}-I_h\boldsymbol{v}\| + |q-J_hq| \leqslant c\,h^k(\|\boldsymbol{v}\|_{k+1} + \|q\|_k)$$

for any $(\boldsymbol{v},q)\in Y\cap(H^{k+1}(\Omega)^d\times H^k(\Omega)), 1\leqslant k\leqslant l$.

(H3) Inverse inequality:

$$\|\boldsymbol{v}_h\| \leqslant ch^{-1}|\boldsymbol{v}_h| \quad \forall\boldsymbol{v}_h\in X_h.$$

(H4) Y_h satisfies the discrete LBB condition:

$$\inf_{q\in M_h}\sup_{v\in X_h}\frac{(q,\operatorname{div}\boldsymbol{v})}{|q|\,\|\boldsymbol{v}\|}\geqslant\beta_0>0.$$

Here $c>0$ is a general constant independent of h.

The following optimal error estimates are well known (cf. [1,2,6,7]):

Theorem 2.1. *Suppose* $(\boldsymbol{u},p)\in Y\cap(H^{k+1}(\Omega)^d,H^k(\Omega))$ *is a nonsingular solution of* (2.2) *and the finite element subspace* Y_h *satisfies assumptions* (H1)–(H4). *Then there exists a solution* $(\boldsymbol{u}_h,p_h)$ *to the Galerkin equation* (2.7) *and we have the following optimal error estimates for certain constant* $c_2>0$ *independent of* h

$$h\|\boldsymbol{u}-\boldsymbol{u}_h\|+|\boldsymbol{u}-\boldsymbol{u}_h|+h|p-p_h|\leqslant c_2h^{k+1}(\|\boldsymbol{u}\|_{k+1}+\|p\|_k). \tag{2.8}$$

3. Projection and lower frequency analysis

Later on, we use the graph norm

$$|||(\boldsymbol{v},q)|||^2=\|\boldsymbol{v}\|^2+|q|^2\quad\forall(\boldsymbol{v},q)\in Y. \tag{3.1}$$

The Navier–Stokes operator $F(\cdot,\cdot)$ is a mapping from Y to Y^* (dual space of Y) defined as follows: for any $(\boldsymbol{u},p)\in Y$,

$$\langle F(\boldsymbol{u},p),(\boldsymbol{v},q)\rangle=a(\boldsymbol{u},\boldsymbol{v})+b(\boldsymbol{u};\boldsymbol{u},\boldsymbol{v})+(q,\operatorname{div}\boldsymbol{u})-(p,\operatorname{div}\boldsymbol{v})-(f,\boldsymbol{v})\quad\forall(\boldsymbol{v},q)\in Y.$$

Then the weak formulation (2.2) is equivalent to

$$F(\boldsymbol{u},p)=0. \tag{3.2}$$

The Frechet derivative operator of $F(\boldsymbol{u},p)$ at $(\boldsymbol{u},p)$ is denoted by $DF(\boldsymbol{u},p)$, which is a linear mapping from Y to Y^* defined by

$$\langle DF(\boldsymbol{u},p)(\boldsymbol{w},r),(\boldsymbol{v},q)\rangle=a(\boldsymbol{w},\boldsymbol{v})+b(\boldsymbol{u};\boldsymbol{w},\boldsymbol{v})+b(\boldsymbol{w};\boldsymbol{u},\boldsymbol{v})+(q,\operatorname{div}\boldsymbol{w})-(r,\operatorname{div}\boldsymbol{v}).$$

For the sake of simplicity, we introduce a bilinear form: $\forall(\boldsymbol{w},r),(\boldsymbol{v},q)\in Y$

$$\mathscr{L}((\boldsymbol{w},r),(\boldsymbol{v},q))=\langle DF(\boldsymbol{u},p)(\boldsymbol{w},r),(\boldsymbol{v},q)\rangle=C_u(\boldsymbol{w},\boldsymbol{v})+(q,\operatorname{div}\boldsymbol{w})-(r,\operatorname{div}\boldsymbol{v}), \tag{3.3}$$

where

$$C_u(\boldsymbol{w},\boldsymbol{v})=a(\boldsymbol{w},\boldsymbol{v})+b(\boldsymbol{u};\boldsymbol{w},\boldsymbol{v})+b(\boldsymbol{w};\boldsymbol{u},\boldsymbol{v}). \tag{3.4}$$

As well known (cf. [6]) that $(\boldsymbol{u},p)$ is a nonsingular solution of (2.2) if and only if $\mathscr{L}(\cdot,\cdot)$ satisfies the inf–sup conditions: there exists a constant $\beta>0$ such that

$$\inf_{(\boldsymbol{w},r)\in Y}\sup_{(\boldsymbol{v},q)\in Y}\frac{\mathscr{L}((\boldsymbol{w},r),(\boldsymbol{v},q))}{|||(\boldsymbol{w},r)|||\,|||(\boldsymbol{v},q)|||},\quad\inf_{(\boldsymbol{v},q)\in Y}\sup_{(\boldsymbol{w},r)\in Y}\frac{\mathscr{L}((\boldsymbol{w},r),(\boldsymbol{v},q))}{|||(\boldsymbol{w},r)|||\,|||(\boldsymbol{v},q)|||}\geqslant\beta. \tag{3.5}$$

Of course, the variational problem: find $(\boldsymbol{w},r)\in Y$ such that

$$\mathscr{L}((\boldsymbol{w},r),(\boldsymbol{v},q))=(\boldsymbol{f},\boldsymbol{v})\quad\forall(\boldsymbol{v},q)\in Y, \tag{3.6}$$

has a unique solution.

The Following lemma describes the conditions which ensure that a point $(\tilde{\boldsymbol{u}},\tilde{p})$ close to a nonsingular point $(\boldsymbol{u},p)$ is also a nonsingular point (cf. [2,6]).

Lemma 3.1. *Assume that* $\tilde{Y}\subset Y$ *is a finite-dimensional subspace and* $\tilde{F}$ *a smooth mapping from* $\tilde{Y}$ *to* Y^*. *Let* $(\boldsymbol{u},p)$ *be a nonsingular point of* $F(\boldsymbol{u},p)$, *and*

$$\sigma(\boldsymbol{u},p) = \|DF(\boldsymbol{u},p)^{-1}\|_{\mathscr{L}(Y^*,Y)}, \tag{3.7}$$

$$\mu(\tilde{\boldsymbol{u}},\tilde{p}) = \|DF(\boldsymbol{u},p) - D\tilde{F}(\tilde{\boldsymbol{u}},\tilde{p})\|_{\mathscr{L}(Y,Y^*)}. \tag{3.8}$$

If $(\tilde{\boldsymbol{u}},\tilde{p})$ *is close to* $(\boldsymbol{u},p)$ *such that*

$$\sigma(\boldsymbol{u},p)\mu(\tilde{\boldsymbol{u}},\tilde{p}) < 1, \tag{3.9}$$

$D\tilde{F}(\tilde{\boldsymbol{u}},\tilde{p})$ *is an isomorphism from* $\tilde{Y}$ *onto* Y^*. *Hence* $(\tilde{\boldsymbol{u}},\tilde{p})$ *is a nonsingular point of* $\tilde{F}$.

Now we denote by $\tilde{F}(\cdot,\cdot)$ the approximate Navier–Stokes operator associate with (2.7). That is

$$\langle\tilde{F}(\boldsymbol{u}_h,p_h),(\boldsymbol{v},q)\rangle = a(\boldsymbol{u}_h,\boldsymbol{v}) + b(\boldsymbol{u}_h;\boldsymbol{u}_h,\boldsymbol{v}) + (q,\operatorname{div}\boldsymbol{u}_h) - (p_h,\operatorname{div}\boldsymbol{v}) - (\boldsymbol{f},\boldsymbol{v}) = 0.$$

From the above lemma and Theorem 2.1, it is obvious that:

Corollary 3.1. *If* $(\boldsymbol{u},p)$ *is a nonsingular solution to* (2.2) *and h is sufficiently small such that*

$$2c_1c_2(\|\boldsymbol{u}\|_2 + \|p\|)h\beta^{-1} < \frac{1}{2}, \tag{3.10}$$

$(\boldsymbol{u}_h,p_h)$ *is also a nonsingular solution to* (2.7).

Later on, we need the Stokes operator and its adjoint operator, which are defined as

$$C_h(\boldsymbol{w},\boldsymbol{v}) = a(\boldsymbol{w},\boldsymbol{v}) + b(\boldsymbol{u}_h;\boldsymbol{w},\boldsymbol{v}) + b(\boldsymbol{w};\boldsymbol{u}_h,\boldsymbol{v}), \quad C_h^*(\boldsymbol{w},\boldsymbol{v}) = C_h(\boldsymbol{v},\boldsymbol{w}).$$

Meanwhile, we introduce the following bilinear form and formal adjoint bilinear forms: for any $(\boldsymbol{w},r),(\boldsymbol{v},q)\in Y$

$$\mathscr{L}_h((\boldsymbol{w},r),(\boldsymbol{v},q)) = C_h(\boldsymbol{w},\boldsymbol{v}) + (q,\operatorname{div}\boldsymbol{w}) - (r,\operatorname{div}\boldsymbol{v}) = \mathscr{L}_h^*((\boldsymbol{v},q),(\boldsymbol{w},r)), \tag{3.11}$$

$$\mathscr{L}^*((\boldsymbol{w},r),(\boldsymbol{v},q)) = \mathscr{L}((\boldsymbol{v},q),(\boldsymbol{w},r)). \tag{3.12}$$

Then we have

$$\langle D\tilde{F}(\boldsymbol{u}_h,p_h)(\boldsymbol{w},r),(\boldsymbol{v},q)\rangle = \mathscr{L}_h((\boldsymbol{w},r),(\boldsymbol{v},q)). \tag{3.13}$$

In the sequel, we will frequently use the following equality:

$$\mathscr{L}_h((\boldsymbol{w},r),(\boldsymbol{v},q)) = \mathscr{L}((\boldsymbol{w},r),(\boldsymbol{v},q)) + b(\boldsymbol{u}_h-\boldsymbol{u};\boldsymbol{w},\boldsymbol{v}) + b(\boldsymbol{w};\boldsymbol{u}_h-\boldsymbol{u},\boldsymbol{v}). \tag{3.14}$$

Thanks to (3.5) and (3.14), if h is small enough such that (3.10) holds, we have

$$\inf_{(\boldsymbol{w},r)\in Y}\sup_{(\boldsymbol{v},q)\in Y}\frac{\mathscr{L}_h((\boldsymbol{w},r),(\boldsymbol{v},q))}{|||(\boldsymbol{w},r)|||\,|||(\boldsymbol{v},q)|||}, \quad \inf_{(\boldsymbol{v},q)\in Y}\sup_{(\boldsymbol{w},r)\in Y}\frac{\mathscr{L}_h((\boldsymbol{w},r),(\boldsymbol{v},q))}{|||(\boldsymbol{w},r)|||\,|||(\boldsymbol{v},q)|||} \geqslant \frac{\beta}{2}. \tag{3.15}$$

On the other hand, by virtue of the corollary, if h satisfies (3.10), there must be certain constant which we will still use the symbol β without loss of generality such that:

$$\inf_{(\boldsymbol{w},r)\in Y_h}\sup_{(\boldsymbol{v},q)\in Y_h}\frac{\mathscr{L}_h((\boldsymbol{w},r),(\boldsymbol{v},q))}{|||(\boldsymbol{w},r)|||\,|||(\boldsymbol{v},q)|||}, \quad \inf_{(\boldsymbol{v},q)\in Y_h}\sup_{(\boldsymbol{w},r)\in Y_h}\frac{\mathscr{L}_h((\boldsymbol{w},r),(\boldsymbol{v},q))}{|||(\boldsymbol{w},r)|||\,|||(\boldsymbol{v},q)|||} \geqslant \frac{\beta}{2}. \tag{3.16}$$

Now, we can define the projection $(Q_h,R_h): Y\to Y_h$ as follows: for any $(\boldsymbol{w},r)\in Y$, find $(Q_h(\boldsymbol{w},r), R_h(\boldsymbol{w},r))\in Y_h$ such that

$$\mathscr{L}_h((\boldsymbol{w}-Q_h(\boldsymbol{w},r), r-R_h(\boldsymbol{w},r)),(\boldsymbol{v},q)) = 0 \quad \forall(\boldsymbol{v},q)\in Y_h. \tag{3.17}$$

By virtue of (3.16) we claim that there exists a unique solution of (3.17). Consequently, the space Y can be splitted into two subspaces:

$$Y = Y_h + \hat{Y}_h.$$

This means that for any $(\boldsymbol{w}, r) \in Y$

$$\boldsymbol{w} = Q_h(\boldsymbol{w}, r) + \hat{\boldsymbol{w}}, \quad r = R_h(\boldsymbol{w}, r) + \hat{r}, \quad (\hat{\boldsymbol{w}}, \hat{r}) \in \hat{Y}_h,$$

where $\hat{Y}_h$ is the orthogonal compliment of Y_h in Y with respect to $\mathscr{L}_h(\cdot,\cdot)$.

By the definition of $\mathscr{L}_h^*(\cdot,\cdot)$, it is easy to see that

$$\mathscr{L}_h^*((\boldsymbol{v}, q), (\hat{\boldsymbol{w}}, \hat{r})) = 0 \quad \forall (\hat{\boldsymbol{w}}, \hat{r}) \in \hat{Y}_h, \ (\boldsymbol{v}, q) \in Y_h. \tag{3.18}$$

We know that Y_h and $\hat{Y}_h$ consist of lower frequency components (large eddy) and higher frequency components (small eddy) in Y respectively. The next lemma shows the higher frequency components is very small.

Lemma 3.2. *Assume that $(\boldsymbol{u}, p)$ is a nonsingular solution of* (2.2) *and the adjoint linearized Navier–Stokes equations: find $(\boldsymbol{w}, r) \in Y$ such that*

$$\mathscr{L}^*((\boldsymbol{w}, r), (\boldsymbol{v}, q)) = (\boldsymbol{f}, \boldsymbol{v}) \quad \forall (\boldsymbol{v}, q) \in Y \tag{3.19}$$

is $H^2(\Omega)$-regular. Furthermore, if the finite element subspace Y_h satisfies the assumptions $(H1)$–$(H4)$, *the projection (Q_h, R_h) defined by* (3.17) *satisfies*:

$$|||(\boldsymbol{w} - Q_h(\boldsymbol{w}, r), r - R_h(\boldsymbol{w}, r))||| \leqslant c_3 |||(\boldsymbol{w}, r)||| \quad \forall (\boldsymbol{w}, r) \in Y, \tag{3.20}$$

$$|||(\hat{\boldsymbol{w}}, \hat{r})||| \leqslant c_4 h^k (\|\boldsymbol{w}\|_{k+1} + \|r\|_k) \quad \forall (\boldsymbol{w}, r) \in Y \cap (H^{k+1}(\Omega)^d \times H^k(\Omega)). \tag{3.21}$$

$$|\hat{\boldsymbol{w}}| \leqslant c_5 h \|\hat{\boldsymbol{w}}\| \quad \forall \boldsymbol{w} \in X. \tag{3.22}$$

$$\|\hat{\boldsymbol{w}}\|_\theta \leqslant c_6 h^{k+1-\theta} (\|\boldsymbol{w}\|_{k+1} + \|r\|_k) \quad \forall (\boldsymbol{w}, r) \in Y \cap (H^{k+1}(\Omega)^d \times H^k(\Omega)), \tag{3.23}$$

where c_3, c_4, c_5, c_6 are positive constants independent of h and will be given in the proof of this lemma, $0 \leqslant \theta \leqslant 1$. (3.22) *is called the enhanced Poincare inequality.*

Proof. Due to the nonsingularity of $(\boldsymbol{u}, p)$, (3.15) and (3.17), we get $\forall (\boldsymbol{w}, r) \in Y$

$$\begin{aligned} |||(Q_h(\boldsymbol{w}, r), R_h(\boldsymbol{w}, r))||| &\leqslant 2\beta^{-1} \sup_{(\boldsymbol{v},q)\in Y} \frac{\mathscr{L}_h((Q_h(\boldsymbol{w}, r), R_h(\boldsymbol{w}, r)), (\boldsymbol{v}, q))}{|||(\boldsymbol{v}, q)|||} \\ &= 2\beta^{-1} \sup_{(\boldsymbol{v},q)\in Y} \frac{\mathscr{L}_h((\boldsymbol{w}, r), (\boldsymbol{v}, q))}{|||(\boldsymbol{v}, q)|||} \leqslant 2\sqrt{2}(\lambda + 2c_1\|\boldsymbol{u}_h\| + 1)\beta^{-1} |||(\boldsymbol{w}, r)|||. \end{aligned}$$

This proves (3.20) by the triangle inequality and $c_3 = 2\sqrt{2}(\lambda + 2c_1\|\boldsymbol{u}_h\| + 1)\beta^{-1} + 1$.

Assume that $(\boldsymbol{\phi}, \lambda)$ is a solution of (3.19) with the right-hand side term $\boldsymbol{f} = \hat{\boldsymbol{w}} \equiv \boldsymbol{w} - Q_h(\boldsymbol{w}, r)$. Thanks to (3.11), (3.12) and (3.14), let $(\boldsymbol{v}, q) = (\hat{\boldsymbol{w}}, \hat{r})$ we can obtain

$$\mathscr{L}_h^*((\boldsymbol{\phi}, \lambda), (\hat{\boldsymbol{w}}, \hat{r})) = |\hat{\boldsymbol{w}}|^2 + b(\boldsymbol{u}_h - \boldsymbol{u}; \hat{\boldsymbol{w}}, \boldsymbol{\phi}) + b(\hat{\boldsymbol{w}}; \boldsymbol{u}_h - \boldsymbol{u}, \boldsymbol{\phi}).$$

Then for any $(\boldsymbol{\phi}_h, \lambda_h) \in Y_h$ and noticing (3.18), we have

$$|\hat{\boldsymbol{w}}|^2 = \mathscr{L}_h^*((\boldsymbol{\phi} - \boldsymbol{\phi}_h, \lambda - \lambda_h), (\hat{\boldsymbol{w}}, \hat{r})) + b(\boldsymbol{u} - \boldsymbol{u}_h; \hat{\boldsymbol{w}}, \boldsymbol{\phi}) + b(\hat{\boldsymbol{w}}; \boldsymbol{u} - \boldsymbol{u}_h, \boldsymbol{\phi}). \tag{3.24}$$

Taking $(\boldsymbol{\phi}_h, \lambda_h) = (I_h\boldsymbol{\phi}, J_h\lambda) \in Y_h$ and using the H^2-regularity of (3.19)

$$\|\boldsymbol{\phi}\|_2 + \|\lambda\| \leqslant c_0|\boldsymbol{f}| = c_0|\hat{\boldsymbol{w}}|,$$

we can derive by (H2) that

$$
\begin{aligned}
|\mathscr{L}_h^*((\boldsymbol{\phi}-\boldsymbol{\phi}_h,\lambda-\lambda_h),(\hat{\boldsymbol{w}},\hat{r}))| &\leqslant \sqrt{2}(\lambda+2c_1\|\boldsymbol{u}_h\|+1)|||(\boldsymbol{\phi}-\boldsymbol{\phi}_h,\lambda-\lambda_h)|||\,|||(\hat{\boldsymbol{w}},\hat{r})||| \\
&\leqslant \sqrt{2}c(\lambda+2c_1\|\boldsymbol{u}_h\|+1)h(\|\boldsymbol{\phi}\|_2+\|\lambda\|)|||(\hat{\boldsymbol{w}},\hat{r})||| \\
&\leqslant \sqrt{2}cc_0(\lambda+2c_1\|\boldsymbol{u}_h\|+1)h|\hat{\boldsymbol{w}}|\,|||(\hat{\boldsymbol{w}},\hat{r})|||.
\end{aligned}
$$

By using Theorem 2.1 and applying (2.5) with $s_1=1$, $s_2=0$, $s_3=2$, we obtain

$$
\begin{aligned}
&|b(\boldsymbol{u}-\boldsymbol{u}_h;\hat{\boldsymbol{w}},\boldsymbol{\phi})| \leqslant c_1\|\boldsymbol{u}_h-\boldsymbol{u}\|\|\boldsymbol{\phi}\|_2\|\hat{\boldsymbol{w}}\| \leqslant c_0c_1c_2(\|\boldsymbol{u}\|_2+\|p\|)h|\hat{\boldsymbol{w}}|\,\|\hat{\boldsymbol{w}}\|, \\
&|b(\hat{\boldsymbol{w}};\boldsymbol{u}-\boldsymbol{u}_h,\boldsymbol{\phi})| \leqslant c_1\|\hat{\boldsymbol{w}}\|\,\|\boldsymbol{u}-\boldsymbol{u}_h\|\,\|\boldsymbol{\phi}\|_2 \leqslant c_0c_1c_2(\|\boldsymbol{u}\|_2+\|p\|)h|\hat{\boldsymbol{w}}|\,\|\hat{\boldsymbol{w}}\|.
\end{aligned}
$$

Combining these relations with (3.24) yields

$$
|\hat{\boldsymbol{w}}| \leqslant [\sqrt{2}cc_0(\lambda+2c_1\|\boldsymbol{u}_h\|+1)+2c_0c_1c_2(\|\boldsymbol{u}\|_2+\|p\|)]h|||(\hat{\boldsymbol{w}},\hat{r})|||.
$$

This proves (3.22) by taking $r=0$ and $c_5=\sqrt{2}cc_0(\lambda+2c_1\|\boldsymbol{u}_h\|+1)+2c_0c_1c_2(\|\boldsymbol{u}\|_2+\|p\|)$.

Now let us estimate $|||(\hat{\boldsymbol{w}},\hat{r})|||$ by using (3.16), (3.17) and (H2) again.

$$
\begin{aligned}
|||(I_h\boldsymbol{w}-Q_h(\boldsymbol{w},r),J_hr-R_h(\boldsymbol{w},r))||| &\leqslant 2\beta^{-1}\sup_{(\boldsymbol{v},q)\in Y_h}\frac{\mathscr{L}_h((I_h\boldsymbol{w}-Q_h(\boldsymbol{w},r),J_hr-R_h(\boldsymbol{w},r)),(\boldsymbol{v},q))}{|||(\boldsymbol{v},q)|||} \\
&\leqslant 2\beta^{-1}\sup_{(\boldsymbol{v},q)\in Y_h}\frac{\mathscr{L}_h((I_h\boldsymbol{w}-\boldsymbol{w},J_hr-r),(\boldsymbol{v},q))}{|||(\boldsymbol{v},q)|||} \\
&\leqslant (c_3-1)|||(I_h\boldsymbol{w}-\boldsymbol{w},J_hr-r)||| \\
&\leqslant c(c_3-1)h^k(\|\boldsymbol{w}\|_{k+1}+\|r\|_k).
\end{aligned}
$$

By the triangle inequality, we obtain

$$
\begin{aligned}
|||(\hat{\boldsymbol{w}},\hat{r})||| &\leqslant |||(\boldsymbol{w}-I_h\boldsymbol{w},r-J_hr)|||+|||(I_h\boldsymbol{w}-Q_h,J_hr-R_h)||| \\
&\leqslant ch^k(\|\boldsymbol{w}\|_{k+1}+\|r\|_k)+c(c_3-1)h^k(\|\boldsymbol{w}\|_{k+1}+\|r\|_k).
\end{aligned}
$$

This proves (3.21) by taking $c_4=cc_3$. Finally (3.23) follows directly from the Sobolev interpolation theory and (3.21), (3.22). □

Having constructed the projection, let us do some lower frequency analysis to show that the distance between the standard Galerkin approximation $(\boldsymbol{u}_h,p_h)$ and the lower frequency components of the true solution is much smaller than that of $(\boldsymbol{u}_h,p_h)$ and $(\boldsymbol{u},p)$, which is very important for constructing our new numerical scheme as said in Section 1.

Set

$$
\boldsymbol{e}=Q_h(\boldsymbol{u},p)-\boldsymbol{u}_h,\quad \varepsilon=R_h(\boldsymbol{u},p)-p_h.
$$

It is easy to see that

$$
\boldsymbol{\eta}=\boldsymbol{u}-\boldsymbol{u}_h=\boldsymbol{e}+\hat{\boldsymbol{u}},\quad \xi=p-p_h=\varepsilon+\hat{p}.
$$

Noticing

$$
b(\boldsymbol{u};\boldsymbol{u},\boldsymbol{v})-b(\boldsymbol{u};\boldsymbol{u}_h,\boldsymbol{v})-b(\boldsymbol{u}_h;\boldsymbol{u},\boldsymbol{v})=b(\boldsymbol{u}-\boldsymbol{u}_h;\boldsymbol{u}-\boldsymbol{u}_h,\boldsymbol{v})-b(\boldsymbol{u}_h;\boldsymbol{u}_h,\boldsymbol{v}),
$$

we can rewrite the Navier–Stokes equations as follows:

$$
\mathscr{L}_h((Q_h,R_h),(\boldsymbol{v},q))+\mathscr{L}_h((\hat{\boldsymbol{u}},\hat{p}),(\boldsymbol{v},q))+b(\boldsymbol{\eta};\boldsymbol{\eta},\boldsymbol{v})-b(\boldsymbol{u}_h;\boldsymbol{u}_h,\boldsymbol{v})=(\boldsymbol{f},\boldsymbol{v}). \tag{3.25}
$$

On the other hand, the Galerkin finite element equations (2.7) can be written as

$$
\mathscr{L}_h((\boldsymbol{u}_h,p_h),(\boldsymbol{v},q))-b(\boldsymbol{u}_h;\boldsymbol{u}_h,\boldsymbol{v})=(\boldsymbol{f},\boldsymbol{v})\quad \forall(\boldsymbol{v},q)\in Y_h. \tag{3.26}
$$

Restricting (3.25) in Y_h, subtracting it from (3.26) and using (3.17), we get

$$\mathscr{L}_h((\boldsymbol{e},\varepsilon),(\boldsymbol{v},q)) + b(\boldsymbol{\eta};\boldsymbol{\eta},\boldsymbol{v}) = 0 \quad \forall(\boldsymbol{v},q)\in Y_h. \tag{3.27}$$

By means of the inf–sup condition (3.16),

$$|||(\boldsymbol{e},\varepsilon)||| \leqslant 2\beta^{-1}\sup_{(\boldsymbol{v},q)\in Y_h}\frac{\mathscr{L}_h((\boldsymbol{e},\varepsilon),(\boldsymbol{v},q))}{|||(\boldsymbol{v},q)|||} \leqslant 2\beta^{-1}\sup_{(\boldsymbol{v},q)\in Y_h}\frac{-b(\boldsymbol{\eta};\boldsymbol{\eta},\boldsymbol{v})}{|||(\boldsymbol{v},q)|||}. \tag{3.28}$$

It follows from (2.4) and (2.5) that

$$|b(\boldsymbol{\eta};\boldsymbol{\eta},\boldsymbol{v})| = |b(\boldsymbol{\eta};\boldsymbol{v},\boldsymbol{\eta})| \leqslant c_1\|\boldsymbol{\eta}\|_{s_1}\|\boldsymbol{\eta}\|_{s_2}\|\boldsymbol{v}\|, \quad s_1+s_2 \geqslant \frac{d}{2}.$$

We take $s_1 = s_2 = 1/2$ for $d=2$, $s_1 = 1/2,\ s_2 = 1$ for $d = 3$ and using the following inequality:

$$|\boldsymbol{\eta}|_{1/2} \leqslant |\boldsymbol{\eta}|^{1/2}\|\boldsymbol{\eta}\|^{1/2},$$

we have

$$|b(\boldsymbol{\eta};\boldsymbol{\eta},\boldsymbol{v})| \leqslant c_1|\boldsymbol{\eta}|^{1-\varepsilon}\|\boldsymbol{\eta}\|^{1+\varepsilon}\|\boldsymbol{v}\|, \tag{3.29}$$

where $\varepsilon = 0$ when $d = 2$, and $\varepsilon = 1/2$ when $d = 3$.

Now it follows from (3.28) and (3.29) that:

Theorem 3.1. *Suppose that* (2.2) *and* (3.19) *are $H^{k+1}(\Omega)$-regular and $H^2(\Omega)$-regular respectively, and the finite element subspace Y_h satisfies the assumptions* ($H1$)–($H4$). *Let $(\boldsymbol{u},p)$ and $(\boldsymbol{u}_h,p_h)$ be the solutions of* (2.2) *and* (2.7) *respectively, and $(\boldsymbol{u},p)$ is nonsingular. (Q_h,R_h) is the projection on Y_h defined by* (3.17). *We have the following error estimate*

$$|||(\boldsymbol{e},\varepsilon)||| \leqslant 2c_1\beta^{-1}\|u-u_h\|^{1+\varepsilon}|u-u_h|^{1-\varepsilon} \leqslant c_7h^{2k+1-\varepsilon},$$

where $\varepsilon = 0$ for $d = 2$, $\varepsilon = 1/2$ for $d = 3$ and $c_7 = c_7(\beta,\|\boldsymbol{u}\|_{k+1},\|p\|_k) > 0$.

4. A new AIM and its related numerical scheme

We know from Section 3 that

$$\|\boldsymbol{u}-\boldsymbol{u}_h\| \leqslant \|Q_h(\boldsymbol{u},p)-\boldsymbol{u}_h+\hat{\boldsymbol{u}}\| \leqslant \|\boldsymbol{e}\| + \|\hat{\boldsymbol{u}}\|,$$

and $\|\boldsymbol{e}\|$ is of higher-order accuracy, but $\|\hat{\boldsymbol{u}}\|$ does not. So, it is the truncated part $(\hat{\boldsymbol{u}},\hat{p})$ in the sense of the projection Q_h that dominates the error between $\boldsymbol{u}_h$ and $\boldsymbol{u}$. If we can obtain a suitable approximation of this truncated part by the known information $(\boldsymbol{u}_h,p_h)$, we may get a more accurate approximation. We are going to introduce an approximate inertial manifold which reflects the approximate interactive relation between the higher and lower frequency components to achieve the goal.

Thanks to (3.25), the alternative form of the Navier–Stokes equations, property (3.17) and noticing

$$\mathscr{L}_h((\boldsymbol{w},r),(\boldsymbol{v},q)) = -\mathscr{L}_h^*((\boldsymbol{w},r),(\boldsymbol{v},q)) + C_h(\boldsymbol{w},\boldsymbol{v}) + C_h(\boldsymbol{v},\boldsymbol{w}), \tag{4.1}$$

we define a new approximate inertial manifold as: for given $(\boldsymbol{w},r)\in Y_h$

$$\begin{cases} \text{find } (\boldsymbol{\phi},\xi) = (\boldsymbol{\phi}(\boldsymbol{w},r),\xi(\boldsymbol{w},r)) \in \hat{Y}_h \quad \text{such that } \forall(\boldsymbol{v},q)\in\hat{Y}_h \\ \mathscr{L}_h((\boldsymbol{\phi},\xi),(\boldsymbol{v},q)) = b(\boldsymbol{w};\boldsymbol{w},\boldsymbol{v}) - C_h(\boldsymbol{w},\boldsymbol{v}) - C_h(\boldsymbol{v},\boldsymbol{w}) + (\boldsymbol{f},\boldsymbol{v}). \end{cases} \tag{4.2}$$

It is obvious that (4.2) can define a single value mapping from Y_h to $\hat{Y}_h$ because of the inf–sup condition (3.15). In fact, it is a mapping from X_h to $\hat{Y}_h$ and possesses some common properties of the approximate inertial manifolds.

Theorem 4.1. *If the conditions in Theorem* 3.1 *are satisfied, the mapping* $\Phi = (\boldsymbol{\phi}, \xi)$ *defined by* (4.2) *has the following properties*:

(i) Φ *is Lipschitz continuous with Lipschitz constant* l

$$|||(\Phi(\boldsymbol{w}_1, r_1) - \Phi(\boldsymbol{w}_2, r_2)||| \leqslant l|||(\boldsymbol{w}_1 - \boldsymbol{w}_2, r_1 - r_2)||| \quad \forall(\boldsymbol{w}_1, r_1), (\boldsymbol{w}_2, r_2) \in Y_h \cap B,$$

where $B = \{(\boldsymbol{w}, r) \in Y : |||(\boldsymbol{w}, r)||| \leqslant \rho\}$ *and* l *is* ρ*-dependent*;

(ii) *the thickness of the manifold* $\mathscr{M} = \mathrm{Graph}(\Phi)$ *is* $\delta = \mathrm{dist}((\boldsymbol{u}, p), \mathscr{M})$:

$$\delta \leqslant c_8 h^{2k+1-\varepsilon}, \tag{4.3}$$

where $\varepsilon = 0$ *for* $d = 2$, $\varepsilon = 1/2$ *for* $d = 3$ *and* $c_8 = c_8(c_7, \|\boldsymbol{u}\|_{k+1}, \|p\|_k, \|\boldsymbol{u}_h\|) > 0$.

Proof. Firstly we prove the Lipschitz continuous. Indeed, let $(\boldsymbol{w}_i, r_i) \in Y_h, i = 1, 2$, taking $(\boldsymbol{w}, r) = (\boldsymbol{w}_i, r_i)$ in (4.2) and denoting

$$\boldsymbol{\phi}_i = \boldsymbol{\phi}(\boldsymbol{w}_i, r_i), \quad \xi_i = \xi(\boldsymbol{w}_i, r_i), \quad \boldsymbol{\chi} = \boldsymbol{\phi}_1 - \boldsymbol{\phi}_2, \quad t = \xi_1 - \xi_2,$$

we obtain

$$\mathscr{L}_h((\boldsymbol{\chi}, t), (\boldsymbol{v}, q)) = b(\boldsymbol{w}_1 - \boldsymbol{w}_2; \boldsymbol{w}_1, \boldsymbol{v}) + b(\boldsymbol{w}_2; \boldsymbol{w}_1 - \boldsymbol{w}_2, \boldsymbol{v}) - C_h(\boldsymbol{w}_1 - \boldsymbol{w}_2, \boldsymbol{v}) - C_h(\boldsymbol{v}, \boldsymbol{w}_1 - \boldsymbol{w}_2).$$

By virtue of inf–sup condition, Lemma 3.1 and (3.17), we claim

$$\begin{aligned} |||(\boldsymbol{\chi}, t)||| &\leqslant 2\beta^{-1} \sup_{(\boldsymbol{v},q)\in Y} \frac{\mathscr{L}_h((\boldsymbol{\chi}, t), (\boldsymbol{v}, q))}{|||(\boldsymbol{v}, q)|||} \\ &\leqslant 2\beta^{-1} \sup_{(\boldsymbol{v},q)\in \hat{Y}_h} \frac{\mathscr{L}_h((\boldsymbol{\chi}, t), (\boldsymbol{v}, q))}{|||(\boldsymbol{v}, q)|||} \\ &\leqslant 4\beta^{-1}(\lambda + 2c_1\|\boldsymbol{u}_h\| + c_1\rho)\|\boldsymbol{w}_1 - \boldsymbol{w}_2\| \triangleq l\|\boldsymbol{w}_1 - \boldsymbol{w}_2\|, \end{aligned}$$

where l depends upon $\|\boldsymbol{u}_h\|$ and ρ.

Next, we make estimation of $\hat{\boldsymbol{e}} = \hat{\boldsymbol{u}} - \boldsymbol{\phi}$, $\hat{\varepsilon} = \hat{p} - \xi$ where

$$\boldsymbol{\phi} = \boldsymbol{\phi}(Q_h(\boldsymbol{u}, p), R_h(\boldsymbol{u}, p)), \quad \xi = \xi(Q_h(\boldsymbol{u}, p), R_h(\boldsymbol{u}, p)).$$

For convenience, we use (Q_h, R_h) to denote $(Q_h(\boldsymbol{u}, p), R_h(\boldsymbol{u}, p))$ in the rest of the proof.

Thanks to (4.1), the Navier–Stokes equations (3.25) can be rewritten as

$$\mathscr{L}_h((\hat{\boldsymbol{u}}, \hat{p}), (\boldsymbol{v}, q)) - \mathscr{L}^*_h((Q_h, R_h), (\boldsymbol{v}, q)) + b(\boldsymbol{\eta}; \boldsymbol{\eta}, \boldsymbol{v}) - b(\boldsymbol{u}_h; \boldsymbol{u}_h, \boldsymbol{v}) + C_h(Q_h, \boldsymbol{v}) + C_h(\boldsymbol{v}, Q_h) = (\boldsymbol{f}, \boldsymbol{v}). \tag{4.4}$$

Taking $(\boldsymbol{w}, r) = (Q_h, R_h)$ in (4.2) leads to

$$\mathscr{L}_h((\boldsymbol{\phi}, \xi), (\boldsymbol{v}, q)) = b(Q_h; Q_h, \boldsymbol{v}) - C_h(Q_h, \boldsymbol{v}) - C_h(\boldsymbol{v}, Q_h) + (\boldsymbol{f}, \boldsymbol{v}) \quad \forall(\boldsymbol{v}, q) \in \hat{Y}_h. \tag{4.5}$$

Subtracting (4.5) from (4.4) and taking into account of (3.18), we obtain

$$\mathscr{L}_h((\hat{\boldsymbol{e}}, \hat{\varepsilon}), (\boldsymbol{v}, q)) = -b(\boldsymbol{\eta}; \boldsymbol{\eta}, \boldsymbol{v}) + b(\boldsymbol{u}_h - Q_h; \boldsymbol{u}_h, \boldsymbol{v}) + b(Q_h, \boldsymbol{u}_h - Q_h, \boldsymbol{v}) \quad \forall(\boldsymbol{v}, q) \in \hat{Y}_h.$$

By virtue of inf–sup condition and noticing (3.17),

$$|||(\hat{\boldsymbol{e}}, \hat{\varepsilon})||| \leqslant 2\beta^{-1} \sup_{(\boldsymbol{v},q)\in Y} \frac{\mathscr{L}_h((\hat{\boldsymbol{e}}, \hat{\varepsilon}), (\boldsymbol{v}, q))}{|||(\boldsymbol{v}, q)|||} \leqslant 2\beta^{-1} \sup_{(\boldsymbol{v},q)\in \hat{Y}_h} \frac{-b(\boldsymbol{\eta}; \boldsymbol{\eta}, \boldsymbol{v}) + b(\boldsymbol{e}; \boldsymbol{u}_h, \boldsymbol{v}) + b(Q_h; \boldsymbol{e}, \boldsymbol{v})}{|||(\boldsymbol{v}, q)|||}.$$

Since

$$|b(\boldsymbol{\eta};\boldsymbol{\eta},\boldsymbol{v})| \leqslant c_1|\boldsymbol{\eta}|^{1-\varepsilon}\|\boldsymbol{\eta}\|^{1+\varepsilon}\|\|\boldsymbol{v}\|,$$

$$\begin{aligned}|b(\boldsymbol{e};\boldsymbol{u}_h,\boldsymbol{v}) + b(Q_h;\boldsymbol{e},\boldsymbol{v})| &= |b(\boldsymbol{e};\boldsymbol{u},\boldsymbol{v}) - b(\boldsymbol{e};\boldsymbol{\eta},\boldsymbol{v}) + b(\boldsymbol{e};\boldsymbol{e},\boldsymbol{v}) - b(\boldsymbol{\eta};\boldsymbol{e},\boldsymbol{v}) + b(\boldsymbol{u};\boldsymbol{e},\boldsymbol{v})| \\ &\leqslant c_1(2\|\boldsymbol{u}\| + 2\|\boldsymbol{\eta}\| + \|\boldsymbol{e}\|)\|\boldsymbol{e}\|\,\|\boldsymbol{v}\|,\end{aligned}$$

by using Theorem 3.1 we obtain

$$|||(\hat{\boldsymbol{e}},\hat{\varepsilon})||| \leqslant 2c_1\beta^{-1}[1 + c_1(2\|\boldsymbol{u}\| + 2\|\boldsymbol{\eta}\| + \|\boldsymbol{e}\|)]|\boldsymbol{\eta}|^{1-\varepsilon}\|\boldsymbol{\eta}\|^{1+\varepsilon} \triangleq c_9|\boldsymbol{\eta}|^{1-\varepsilon}\|\boldsymbol{\eta}\|^{1+\varepsilon}. \tag{4.6}$$

This yields (ii). □

From the above Theorem 4.1, the very natural way to correct the standard Galerkin solution is to use the AIM defined by (4.2) to generate a suitable approximation of the truncated part. We summarize this ideal into following scheme:

Step 1. Solve (2.7) to get the standard Galerkin approximation $(\boldsymbol{u}_h, p_h)$.

Step 2. Take $(\boldsymbol{w}, r) = (\boldsymbol{u}_h, p_h)$ in (4.2) to derive $(\boldsymbol{\phi}_h, \xi_h) = \Phi(\boldsymbol{u}_h, p_h)$ which is a suitable approximation to the truncated part $(\hat{\boldsymbol{u}}, \hat{p})$:

$$\mathscr{L}_h((\boldsymbol{\phi}_h,\xi_h),(\boldsymbol{v},q)) = -2a(\boldsymbol{u}_h,\boldsymbol{v}) + (\boldsymbol{f},\boldsymbol{v}) \quad \forall(\boldsymbol{v},q) \in \hat{Y}_h.$$

Step 3. Obtain the corrected approximation

$$(\boldsymbol{u}_*, p_*) = (\boldsymbol{u}_h, p_h) + (\boldsymbol{\phi}_h, \xi_h). \tag{4.7}$$

Using the similar method in the proof of Theorem 4.1, we can easily get:

Theorem 4.2. *Suppose that assumptions of Theorem* 4.1 *hold. Then the above scheme admits*

$$|||(\boldsymbol{u} - \boldsymbol{u}_*, p - p_*)||| \leqslant (2c_1\beta^{-1} + c_9)\|\boldsymbol{u} - \boldsymbol{u}_h\|^{1+\varepsilon}|\boldsymbol{u} - \boldsymbol{u}_h|^{1-\varepsilon} \leqslant (c_8 + c_7)h^{2k+1-\varepsilon},$$

where $\varepsilon = 0$ for $d = 2$ and $\varepsilon = 1/2$ for $d = 3$.

5. On the completion and a one-step Newtonian scheme

Although Theorem 4.2 shows that the scheme (Steps 1–3) possesses much higher convergence rate than the standard Galerkin method, it is not a practical numerical scheme because the construction of the subspace $\hat{Y}_h$ is quite difficult. And it is obviously a time-consuming procedure which may use much more CPU time than solving the Navier–Stokes equations by the standard Galerkin method. In this section, we will give another alternative form of the scheme to make it a high performance practical numerical scheme.

Noticing the definition of $(\boldsymbol{u}_*, p_*)$ in (4.7), we rewrite the equations in Step 2 as

$$\mathscr{L}_h((\boldsymbol{u}_*,p_*),(\boldsymbol{v},q)) - \mathscr{L}_h((\boldsymbol{u}_h,p_h),(\boldsymbol{v},q)) + C_h(\boldsymbol{u}_h,\boldsymbol{v}) + C_h(\boldsymbol{v},\boldsymbol{u}_h) = (\boldsymbol{f},\boldsymbol{v}) + b(\boldsymbol{u}_h;\boldsymbol{u}_h,\boldsymbol{v}) \quad \forall(\boldsymbol{v},q) \in \hat{Y}_h.$$

By using (4.1), the above equations admit

$$\mathscr{L}_h((\boldsymbol{u}_*,p_*),(\boldsymbol{v},q)) + \mathscr{L}_h^*((\boldsymbol{u}_h,p_h),(\boldsymbol{v},q)) = (\boldsymbol{f},\boldsymbol{v}) + b(\boldsymbol{u}_h;\boldsymbol{u}_h,\boldsymbol{v}) \quad \forall(\boldsymbol{v},q) \in \hat{Y}_h.$$

Thanks to (3.18), we can get

$$\mathscr{L}_h((\boldsymbol{u}_*,p_*),(\boldsymbol{v},q)) = (\boldsymbol{f},\boldsymbol{v}) + b(\boldsymbol{u}_h;\boldsymbol{u}_h,\boldsymbol{v}) \quad \forall(\boldsymbol{v},q) \in \hat{Y}_h. \tag{5.1}$$

Because of $(\boldsymbol{\phi}, \xi) \in \hat{Y}_h$ and the standard Galerkin equations (3.26), we have

$$\mathscr{L}_h((\boldsymbol{u}_*,p_*),(\boldsymbol{v},q)) = (\boldsymbol{f},\boldsymbol{v}) + b(\boldsymbol{u}_h;\boldsymbol{u}_h,\boldsymbol{v}) \quad \forall(\boldsymbol{v},q) \in Y_h. \tag{5.2}$$

This is an equivalent form of (3.26). Plus (5.1) and (5.2), we finally can derive the following equations satisfied by $(\boldsymbol{u}_*, p_*) \in Y$:

$$\begin{cases} \text{find } (\boldsymbol{u}_*, p_*) \in Y \quad \text{such that} \\ \mathscr{L}_h((\boldsymbol{u}_*, p_*), (\boldsymbol{v}, q)) = (\boldsymbol{f}, \boldsymbol{v}) + b(\boldsymbol{u}_h; \boldsymbol{u}_h, \boldsymbol{v}) \quad \forall (\boldsymbol{v}, q) \in Y. \end{cases} \tag{5.3}$$

This leads to:

Theorem 5.1. *Assume that* $(\boldsymbol{u}_*, p_*)$ *is a certain approximate solution defined by* (4.7). $(\boldsymbol{u}_*, p_*)$ *satisfies the linearized equations of the Navier–Stokes equations* (5.3) *at* $(\boldsymbol{u}_h, p_h)$.

Therefore, (Step 1) and (5.3) form an equivalent algorithm of Steps 1–3 which certainly share the same convergence results given in Theorem 4.2.

It is obvious that the new algorithm avoids solving the higher frequency approximation $(\boldsymbol{\phi}_h, \xi_h)$ in Step 2 in the high frequency subspace $\hat{Y}$ and obtains the final approximate solution $(\boldsymbol{u}_*, p_*)$ by solving a linear equation. So we do not have to construct $\hat{Y}$ in practical and it is much more easier to be carried out than the former algorithm without introducing much extra procedure. This makes it a more practical algorithm.

Till now, we have to solve (5.3) in the whole space Y. In practice, we have to restrict (5.3) in another finite element subspace Y_{h_*} whose mesh size h_* should be much smaller than h. That is, the finite element approximate solution of (5.3) is

$$\begin{cases} \text{find } (\boldsymbol{u}_{h_*}, p_{h_*}) \in Y_{h_*} \quad \text{such that} \\ \mathscr{L}_h((\boldsymbol{u}_{h_*}, p_{h_*}), (\boldsymbol{v}, q)) = (\boldsymbol{f}, \boldsymbol{v}) + b(\boldsymbol{u}_h; \boldsymbol{u}_h, \boldsymbol{v}) \quad \forall (\boldsymbol{v}, q) \in Y_{h_*}. \end{cases} \tag{5.4}$$

(Step 1) together with (5.4) is the final version of our algorithm. Thanks to (H2) and Theorem 4.2, we can easily derive the convergence results of the final algorithm.

Theorem 5.2. *Suppose that assumptions of Theorem* 4.1 *hold. Then the final numerical algorithm admits*

$$|||(\boldsymbol{u} - \boldsymbol{u}_{h_*}, p - p_{h_*})||| \leqslant (c_8 + c_7) h^{2k+1-\varepsilon} + c_{10} h_*^k,$$

where $\varepsilon = 0$ *for* $d = 2$, $\varepsilon = 1/2$ *for* $d = 3$ *and* $c_{10} > 0$ *is a constant independent of* h_* *and* h.

It is very interesting that we can show the numerical scheme (Step 1) and (5.3) derived by the new approximate inertial manifold (4.2) is equivalent a Newton iterative step. In fact, the Newton iterative scheme for solving the Navier–Stokes equations (3.2) are as follows: for certain given initial value $(\boldsymbol{u}_0, p_0) \in Y$, suppose $(\boldsymbol{u}_k, p_k) \in Y$ is known, find $(\boldsymbol{u}_{k+1}, p_{k+1}) \in Y$ such that

$$\langle DF(\boldsymbol{u}_k, p_k)((\boldsymbol{u}_{k+1}, p_{k+1}) - (\boldsymbol{u}_k, p_k)), (\boldsymbol{v}, q)\rangle = -\langle F(\boldsymbol{u}_k, p_k), (\boldsymbol{v}, q)\rangle \quad \forall (\boldsymbol{v}, q) \in Y.$$

By simple calculation, we can easily know that the first Newton iterative step of the above Newton iterative method with initial value $(\boldsymbol{u}_0, p_0) = (\boldsymbol{u}_h, p_h)$ is equivalent to the equations of $(\boldsymbol{u}_*, p_*)$ in (5.3). If we restrict the above procedure in Y_{h_*}, we can get the equations of $(\boldsymbol{u}_{h_*}, p_{h_*})$ in (5.4). So the numerical scheme (Step 1), (5.3) and (Step 1), (5.4) are equivalent to a one step Newton procedure. That also indicates the reason why our AIM-based scheme processes such a high convergence rate.

The proof of Theorem 5.2 is based upon the property of the new Inertial Manifold which was constructed in Section 4. Now we prove this theorem again by the Newton iterative approach.

Another Proof of Theorem 5.2. The proof by the approach of Newton method is quite simple. Notice (3.25), the Navier–Stokes equations are equivalent to

$$\mathscr{L}_h((\boldsymbol{u}, p), (\boldsymbol{v}, q)) = (\boldsymbol{f}, \boldsymbol{v}) + b(\boldsymbol{u}_h; \boldsymbol{u}_h, \boldsymbol{v}) - b(\boldsymbol{\eta}; \boldsymbol{\eta}, \boldsymbol{v}) \quad \forall (\boldsymbol{v}, q) \in Y. \tag{5.5}$$

Now subtracting (5.3) from (5.5) yields

$$\mathscr{L}_h((\boldsymbol{u} - \boldsymbol{u}_*, p - p_*), (\boldsymbol{v}, q)) = -b(\boldsymbol{\eta}; \boldsymbol{\eta}, \boldsymbol{v}) \quad \forall (\boldsymbol{v}, q) \in Y.$$

Under the assumptions of the theorem, (3.15) is valid. Therefore, we have

$$|||(\boldsymbol{u}-\boldsymbol{u}_*, p-p_*)||| \leqslant \frac{2}{\beta} \sup_{(v,q)\in Y} \frac{\mathscr{L}_h((\boldsymbol{u}-\boldsymbol{u}_*, p-p_*),(\boldsymbol{v},q))}{|||(\boldsymbol{v},q)|||} \leqslant \frac{2}{\beta} \sup_{(v,q)\in Y} \frac{-b(\boldsymbol{\eta};\boldsymbol{\eta},\boldsymbol{v})}{|||(\boldsymbol{v},q)|||}.$$

Notice (3.29), we have

$$|||(\boldsymbol{u}-\boldsymbol{u}_*, p-p_*)||| \leqslant 2c_1\beta^{-1}|\boldsymbol{\eta}|^{1-\varepsilon}\|\boldsymbol{\eta}\|^{1+\varepsilon},$$

here $\varepsilon = 0$ for $d = 2$ and $\varepsilon = 1/2$ for $d = 3$. □

Remark 2. If we take $k = 1$ in Theorem 5.2, we have

$$|||(\boldsymbol{u},p)-(\boldsymbol{u}_{h_*},p_{h_*})||| \leqslant c(h^3+h_*), \quad d=2,$$
$$|||(\boldsymbol{u},p)-(\boldsymbol{u}_{h_*},p_{h_*})||| \leqslant c(h^{3-\frac{1}{2}}+h_*), \quad d=3.$$

Let us focus our attention on 2D case. To balance the two error terms, we have to choose h_* sufficient small such that

$$h_* \sim h^3. \tag{5.6}$$

That is, we have to solve the standard Galerkin equations (2.7) in Y_h, which is a nonlinear problem and need to be solved by some iterative method, for example, the Newton method. Then we only need to solve a linear system (5.4) in the large subspace Y_{h_*}. According to (5.6), Y_h is a very small subspace compared with Y_{h_*} and its Newton iterative procedure may reach a limit much more quickly than the same procedure in Y_{h_*}. Actually, we will show that the CPU time used by it can be considered negligible compared with one Newton step in Y_{h_*} for h is not very small. So, the CPU time used by our algorithm (Step 1) and (5.4) is almost the CPU time used by one Newton iterative step in Y_{h_*}. Hence, it is a high performance algorithm compared with the standard Galerkin method.

On the other hand, we know that for usual nonlinear Galerkin scheme,

$$|||(\boldsymbol{u},p)-(\boldsymbol{u}_N,p_N)||| \leqslant c(h^2+h_*), \quad d=2.$$

where $(\boldsymbol{u}_N,p_N)$ is the usual nonlinear Galerkin approximation and $h_* \sim h^2$ in order to balance the two error terms. Obviously, our one-step Newton method scheme (Step 1) and (5.4) can improve the accuracy of the standard Galerkin solution much better.

6. Numerical test

This section gives two illustration examples, which verify the high performance of the one-step Newton method (Step 1) and (5.4) (denoted by 1NM in the following).

The first one is a test problem in [4]. With $\Omega = (0,1)\times(0,1) \in \mathscr{R}^2$, the right-hand side term f is chosen such that the exact solution $\boldsymbol{u} = (u_1,u_2)$ and p of (2.2) is given by

$$u_1(x,y) = 2(1-x)(1-x)x^2(1-2y)(1-y)y,$$
$$u_2(x,y) = -2(1-y)(1-y)y^2(1-2x)(1-x)x,$$
$$p = (1-x)x(1-y)y - 25/9.$$

This solution satisfies the homogeneous boundary conditions. We will numerically solve this particular problem by 1NM and other two Newton type methods which are standard Newton method (NM) and Quasi-Newton method (QMN). We use square mesh and 4-point linear element. For 1NM, $h = 1/4$ is the coarse mesh size and $h_* = h^3 = 1/64$ the fine mesh size. We use QNM on coarse mesh to derive the standard Galerkin approximate solution by solving (2.7) while using (5.4) to get the final approximate solution on fine mesh. To compare with the performance of 1NM, we use NM and QNM on the same fine mesh (h_*) to get the approximate solution. For each possible iterative procedure, we use the solution of the related

Stokes equations as the initial value. Noticing the results in Theorem 2.1 and $h_* = h^3$, 1NM will generate the approximate solutions of the Navier–Stokes equations of almost the same accuracy as the standard Galerkin method (NM or QNM). By comparing the CPU time used by these three algorithms, the efficiency of our algorithms is obvious. In the following table, the first three rows indicate the error and the rest three rows indicate the CPU time used by the three algorithms with respect to different viscosity varying from 10^{-1} to 10^{-7}.

v	10^{-1}	10^{-2}	10^{-3}	10^{-4}	10^{-5}	10^{-6}	10^{-7}
NM (error)	1.73−E3	1.71−E3	1.70−E3	1.38−E3	1.08−E3	9.58−E4	8.77−E4
QNM (error)	1.80−E3	1.74−E3	1.70−E3	1.38−E3	1.08−E3	9.60−E4	9.58−E4
1NM (error)	1.71−E3	1.71−E3	1.68−E3	1.19−E3	8.63−E4	1.19−E4	8.38−E4
NM (time)	126.8 s	128.9 s	169.9 s	209.1 s	377.8 s	547.5 s	887.7 s
QNM (time)	120.8 s	123.0 s	124.9 s	131.2 s	225.9 s	320.2 s	401.6 s
1NM (time)	84.9 s	84.9 s	85.6 s	85.4 s	84.6 s	84.8 s	85.9 s

From the above table, it is easy to find that 1NM can reach the same accuracy of the standard Galerkin method (NM and QNM) on the fine mesh h_*. On the other hand, as we said in Remark 2 in the previous section, the CPU time used by 1NM should be almost the same as that of one-step NM and QNM. So 1NM should be more efficient than NM and QNM especially for small v because their iterative procedures may take more and more steps to reach a limit when the viscosity become smaller and smaller. The CPU time in the above table just verifies this. The reason why the CPU time used by QNM is less than that of NM is that NM has to update the stiff matrix on each iterative step while the QNM just has to update it on certain steps.

The second example is a more realistic problem, the axisymmetric spherical Couette–Taylor Flow between two rotating concentric spheres. The data of the problem are

$$R_1 = 1.0, \quad R_2 = 1.18, \quad \omega_1 = 2.0, \quad \omega_2 = 0.0,$$

where R and ω stand for radius and angle speed of the two spheres respectively (see Fig. 1). This is indeed a two-dimensional problem. We only numerically solve it on the right half of the meridian plane ($\phi = \pi/2$). Following are the graphs of the computed streamlines on this plane with respect to different Reynolds numbers, where they are computed by using 8-point isoparametric element on square mesh. For each figure, the left one is the computing result of NM on the coarse grid ($8 \times 32 = 256$ elements), the right one

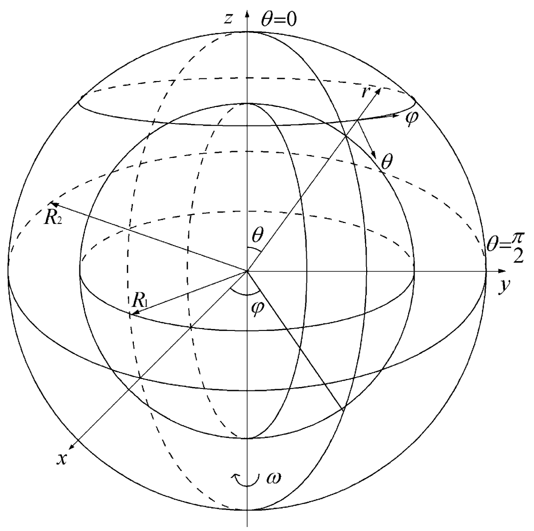

Fig. 1.

is the result of NM on the fine grid ($16 \times 64 = 1024$ elements) and the middle one is the result of 1NM ($16 \times 64 = 1024$ elements) based on the result of the left one. In Figs. 2–4, we use Max_I and CPU_I, $I = 1, 2, 3$ to stand for the maximum value of the computed stream function and the CPU time used by the corresponding scheme.

It is obvious that 1NM can save a lot of CPU time. Comparing the maximum values of the stream functions, we find that 1NM results are more closed to the NM results on fine grid. And the structures of the streamlines of 1NM look more like that of NM on fine grid.

$$Re = 300.00: \left\{\begin{array}{l} Max_1 = 6.6432\mathrm{e}-3, \\ Max_2 = 6.6628\mathrm{e}-3, \\ Max_3 = 6.6639\mathrm{e}-3. \end{array}\right. \left\{\begin{array}{l} CPU_1 = 9.87s, \\ CPU_2 = 22.01s, \\ CPU_3 = 149.91s. \end{array}\right.$$

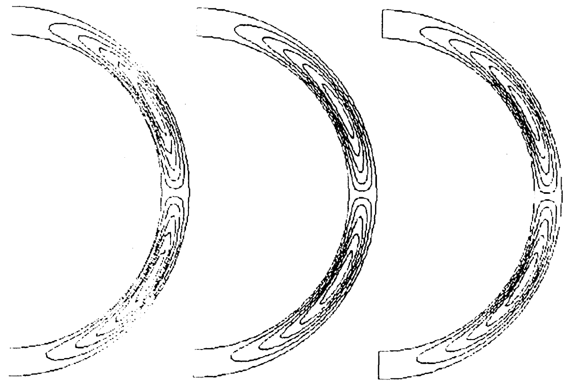

Fig. 2.

$$Re = 350.00: \left\{\begin{array}{l} Max_1 = 7.8288\mathrm{e}-3, \\ Max_2 = 8.8361\mathrm{e}-3, \\ Max_3 = 8.7745\mathrm{e}-3. \end{array}\right. \left\{\begin{array}{l} CPU_1 = 10.82s, \\ CPU_2 = 23.22s, \\ CPU_3 = 183.08s. \end{array}\right.$$

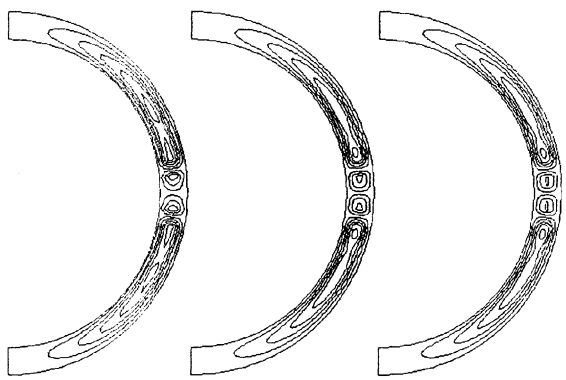

Fig. 3.

$$Re = 400.00: \left\{\begin{array}{l} Max_1 = 1.0274\mathrm{e}-2, \\ Max_2 = 1.1185\mathrm{e}-2, \\ Max_3 = 1.1121\mathrm{e}-2. \end{array}\right. \left\{\begin{array}{l} CPU_1 = 13.62s, \\ CPU_2 = 25.40s, \\ CPU_3 = 456.71s. \end{array}\right.$$

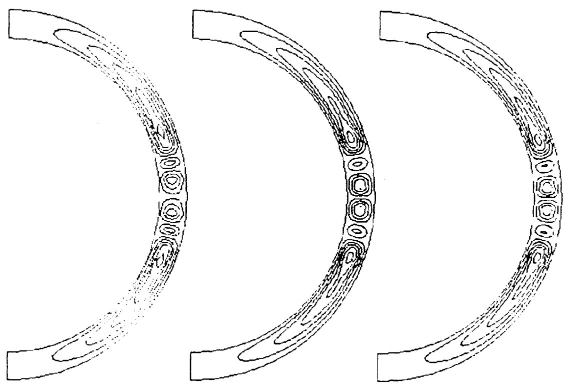

Fig. 4.

7. Conclusion

The numerical examples show that 1NM can get an approximate solution of the Navier–Stokes equations with almost the same accuracy as the approximate solutions derived by the standard Galerkin method (NM and QNM) which are solved on the same fine grid. But the CPU time used by 1NM is much less than them especially for small viscosity (or large Reynolds number). So the 1NM is a high performance numerical scheme.

There still is one thing that should be mentioned. That is the 1NM is developed only for numerical simulating the nonsingular solutions of the steady Navier–Stokes equations. This may restrict the applicable range of our ideal. For the singular case and unsteady problem, we will try to construct new schemes based on the this kind of ideal elsewhere.

References

[1] M. Ainsworth, J.T. Oden, A unified approach to a posteriori error estimation using element residual method, Numer. Math. 23 (1993) 65.
[2] F. Bezzi, M. Fortin, Mixed and Hybrid Finite Element Methods, Springer, New York, 1991.
[3] P. Constantine, C. Foias, Navier–Stokes Equations, Chicago Lecture in Mathematics, University of Chicago, 1988.
[4] V. Ervin, W. Layton, J. Maubach, A posteriori error estimators for a two-level finite element method for the Navier–Stokes equations, Numer. Methods Partial Differential Equations (12) (1996) 333–346.
[5] B. Garcia-Achilla, J. Novo, E. Titi, An approximate inertial manifolds approach to postprocessing the Galerkin method for the Navier–Stokes equations, Math. Comput. 68 (1999) 893–911.
[6] V. Girault, P.-A. Raviart, Finite Element Methods for the Navier–Stokes Equations, Theory and Algorithms, Springer, Berlin, 1986.
[7] M. Gunzburger, Finite Element Methods for Viscous Incompressible Flow, A Guide to Theory, Practice and Algorithms, Academic Press, Boston, 1989.
[8] W. Layton, H.W.J. Lenferink, Two-level picad, defect correction for the Navier–Stokes equations, Appl. Math. Computing 80 (1995) 1–12.
[9] W. Layton, H.W.J. Lenferink, A multilevel mesh independence principle for the Navier–Stokes equations, SIAM J. Numer. Anal. 33 (1996) 11–30.
[10] Q. Lin, Higher Order Accuracy Finite Element Method, Hebei University Press, 1997.
[11] M. Marion, R. Temam, Nonlinear Galerkin methods, SIAM J. Numer. Anal. 26 (1989) 1139–1157.
[12] M. Marion, J. Xu, Error estimates on a new nonlinear Galerkin method based on two-grid finite elements, SIAM J. Numer. Anal. 32 (1995) 1170–1184.
[13] J. Xu, A novel two-grad method for semilinear elliptic equations, SIAM J. Scientific Computing 15 (1994) 231–237.
[14] J. Xu, Two-grid discretization techniques for linear and nonlinear PDEs, SIAM J. Numer. Anal. 33 (1996) 1759–1777.